SciPost Phys. Proc. 8, 066 (2022)

Hard exclusive $\pi^+ n$ electro production beam spin asymmetries off the proton in the GPD and TDA regimes

Stefan Diehl[1,2⋆] for the CLAS collaboration

1 II. Physikalisches Institut der Universität Gießen, 35392 Gießen, Germany
2 University of Connecticut, Storrs, Connecticut 06269, USA

⋆ stefan.diehl@exp2.physik.uni-giessen.de

Proceedings for the XXVIII International Workshop on Deep-Inelastic Scattering and Related Subjects, Stony Brook University, New York, USA, 12-16 April 2021
doi:10.21468/SciPostPhysProc.8

Abstract

Hard exclusive π^+n electro-production can be used to gain access to the 3D nucleon structure. The QCD factorisation mechanism in the "nearly forward region" (t/Q^2 small) allows a description by Generalized Parton Distributions (GPDs), while for the "nearly backward" kinematic region (u/Q^2 small) a description based on nucleon to pion transitions (TDAs) is available. The paper presents a measurement of single beam spin asymmetries to extract the $A_{LU}^{\sin\phi}$ moments and the related cross section ratio $\sigma_{LT'}/\sigma_0$ from the hard exclusive π^+ channel off the unpolarized hydrogen target in a wide range of kinematics based on data taken with the CLAS spectrometer at Jefferson Lab. In addition, under forward angles a detailed multidimensional study will be presented based on CLAS12 data and compared to theoretical predictions.

Received 10-06-2021
Accepted 06-05-2022
Published 12-07-2022
Check for updates
doi:10.21468/SciPostPhysProc.8.066

1 Introduction

Hard exclusive pseudoscalar meson production can be used to study the 3D nucleon structure in terms of the transverse position and the longitudinal momentum component. Applying QCD factorisation, the process in the "nearly forward region" (t/Q^2 small) can be divided into a hard part, described by perturbative QCD and in two general structure functions, the Generalized Parton Distributions (GPDs) for the nucleon and the pion distribution amplitudes (DAs), describing the complex non perturbative structure of these particles [1–3]. Depending on the polarisation of the quarks and the nucleon, there are in total eight GPDs, of which four are chiral-even and four chiral-odd. While the chiral-even GPDs (H, $\widetilde{H}$, E and $\widetilde{E}$) can be well accessed by deeply virtual Compton scattering (DVCS), pseudoscalar meson production can be used to probe also the chiral-odd GPDs (H_T, $\widetilde{H}_T$, E_T, and $\widetilde{E}_T$) [4–6].

In the "nearly backward" kinematic region (u/Q^2 small) a collinear factorized description in terms of a convolution of the non-perturbative nucleon to pion transitions (TDAs), the nucleon DAs and the hard interaction amplitude from pQCD is assumed to be valid [7–10]. Nucleon-to-meson TDAs are universal functions that parametrize the non-perturbative structure of these hadrons. Within the TDA mechanism, the three-quark core of the target nucleon absorbs most of the virtual photon momentum and recoils forward, while a low momentum pion is emitted under backward angles. This process allows us to get new insights into the hadronic structure and to probe non-minimal Fock components of hadronic light-cone wave functions. Recent publications on exclusive π^+ electro-production [11] and on ω electro-production [12] in backward kinematics, provided first indications for the applicability of the TDA mechanism.

The reaction mechanisms in the GPD and TDA regimes are compared in Fig. 1.

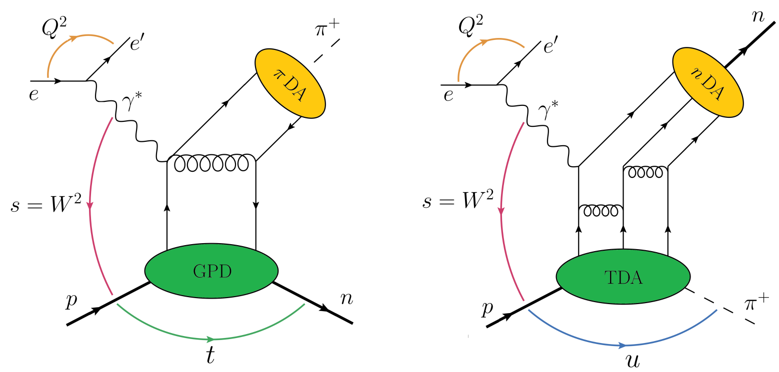

Figure 1: Left: Diagram of the GPD mechanism in very forward kinematics ($-t/Q^2 \ll 1$). Right: Diagram of the TDA mechanism in very backward kinematics ($-u/Q^2 \ll 1$). [13]

For exclusive meson production, GPDs and TDAs can be accessed through different observables, such as differential cross sections and beam and target polarization asymmetries [14, 15]. The focus of this work is on the extraction of the $A_{LU}^{\sin\phi}$ moment and the related cross section ratio $\sigma_{LT'}/\sigma_0$ from beam-spin asymmetries. According to [14], the beam-spin asymmetry can be defined as:

$$BSA(t,\phi,x_B,Q^2) = \frac{d\sigma^+ - d\sigma^-}{d\sigma^+ + d\sigma^-} = \frac{A_{LU}^{\sin\phi}\sin\phi}{1 + A_{UU}^{\cos\phi}\cos\phi + A_{UU}^{\cos 2\phi}\cos 2\phi}, \tag{1}$$

where $d\sigma^\pm$ is the differential cross section for the two beam helicity states ($\pm$). The subscripts ij represent the longitudinal (L) or unpolarized (U) state of the beam and the target and ϕ is the azimuthal angle between the electron scattering and the hadron production plane. The moments $A_{LU}^{\sin\phi}$, $A_{UU}^{\cos\phi}$ and $A_{UU}^{\cos 2\phi}$ can be directly related to the ratio of the interference cross sections $\sigma_{LT'}$, σ_{LT}, σ_{TT} and the non ϕ dependent part of the cross section $\sigma_0 = \sigma_T + \epsilon\sigma_L$ [16]:

$$A_{LU}^{\sin\phi} = \sqrt{2\epsilon(1-\epsilon)}\frac{\sigma_{LT'}}{\sigma_0}, \quad A_{UU}^{\cos\phi} = \sqrt{2\epsilon(1+\epsilon)}\,\frac{\sigma_{LT}}{\sigma_0}, \quad A_{UU}^{\cos 2\phi} = \epsilon\,\frac{\sigma_{TT}}{\sigma_0} \tag{2}$$

where the structure functions σ_L and σ_T correspond to transverse (T) and longitudinal (L) polarized virtual photons. The ratio of their fluxes is given by ϵ, which is determined by the electron scattering kinematics.

The Golskokov-Kroll (GK) model [17] can be used to describe $\sigma_{LT'}$ in terms of GPDs. The model includes chiral-odd GPDs to calculate the contributions from the transversely polarized virtual photon amplitudes [17]. The GPDs are constructed from double distributions and constrained by results from lattice QCD and transversity parton distribution functions [17]. The pion pole contribution to the amplitudes is taken into account. An expression for $\sigma_{LT'}$ is provided through the convolutions of GPDs with sub-process amplitudes (see Fig. 1 left) and contains the products of chiral-odd and chiral-even GPDs [4]: $\sigma_{LT'} \sim Im\left[\langle \overline{E}_T\rangle^* \langle \widetilde{H}\rangle + \langle H_T\rangle^* \langle \widetilde{E}\rangle\right]$, where all involved GPDs are influenced directly or indirectly by the pion pole term (i.e. $\widetilde{E}_{eff} = \widetilde{E}$ + pole), which significantly amplifies the imaginary part of small chiral-odd GPDs in the case of π^+ [13]. Due to the quark composition of π^+ and the resulting wave function, it can be also assumed that $\langle \overline{E}_T\rangle$ is small. Therefore, $\sigma_{LT'}$ is dominated by $Im[\langle H_T\rangle^* \langle \widetilde{E}\rangle]$ for π^+.

In the backward regime a similar expression of $\sigma_{LT'}$ can be found within the TDA model through the interference between the leading twist transverse amplitude of the convolution in terms of twist-3 πN TDAs and nucleon DAs and the next leading sub-process longitudinal amplitude of the convolution involving twist-4 TDAs and DAs [13]. However, a complete theoretical study of this twist-4 longitudinal amplitude is not yet available.

2 Extraction of beam spin asymmetries over a wide range of kinematics with CLAS

A first study of hard exclusive π^+ electro-production beam spin asymmetry over a wide range of kinematics, was performed at Jefferson Lab with the CEBAF Large Acceptance Spectrometer (CLAS) [18]. This work is published in Ref. [13]. The study used a longitudinally polarized electron beam with an energy of 5.498 GeV interacting with a unpolarized liquid hydrogen target. For the selection of deeply inelastic scattered electrons, cuts on $Q^2 > 1$ GeV^2 and on the invariant mass of the hadronic final state $W > 2$ GeV were applied. The exclusive $e'\pi^+ n$ final state, was selcted from the detected electrons and π^+ by a cut around the neutron peak in the $e\pi^+ X$ missing mass spectrum.

Experimentally the BSA and its statistical uncertainty are defined with the number of counts with positive and negative helicity ($N_i^{\pm}$), in a specific bin i as:

$$BSA = \frac{1}{P_b}\frac{N_i^+ - N_i^-}{N_i^+ + N_i^-}\,, \quad \sigma_{BSA} = \frac{2}{P_b}\sqrt{\frac{N_i^+ N_i^-}{(N_i^+ + N_i^-)^3}}, \tag{3}$$

where $P_b = 74.9 \pm 2.4\%$ (stat.) $\pm$ 3.0% (sys.) is the magnitude of the beam polarization. A fit to the ϕ dependence of the BSA, following Eq. (1) was applied to extract the $A_{LU}^{\sin\phi}$ moment. The asymmetry of the background has been subtracted on a bin by bin basis. Several sources of systematic uncertainty were investigated, including particle identification, background subtraction, beam polarization, and the influence of the $A_{UU}^{\cos\phi}$ and $A_{UU}^{\cos 2\phi}$ moments. The impact of acceptance effects was estimated based on Monte Carlo simulations. More details can be found in Ref. [13].

$A_{LU}^{\sin\phi}$ was extracted over the complete range of $-t$ up to 6.6 GeV^2 as shown in Fig. 2, which is close to the maximal accessible $-t$ value. The data is integrated over Q^2, ranging from 1 GeV^2 - 4.5 GeV^2 and x_B ranging from 0.1 to 0.6. Fig. 2 clearly shows, that the t-dependence of $A_{LU}^{\sin\phi}$ makes a transition from positive values in the forward region (small -t) to negative values in the backward region (large -t, small -u) [13]. The sign change occurs around $-t = 3$ GeV^2, which corresponds to 90 degrees in the center of mass frame, and marks the transition between the π^+ emitted in the forward and backward directions. Therefore, the sign change may indicate a transition between the GPD and TDA regimes [13]. Additional studies showed, that the sign change occurs in the complete accessible Q^2 and x_B region [13].

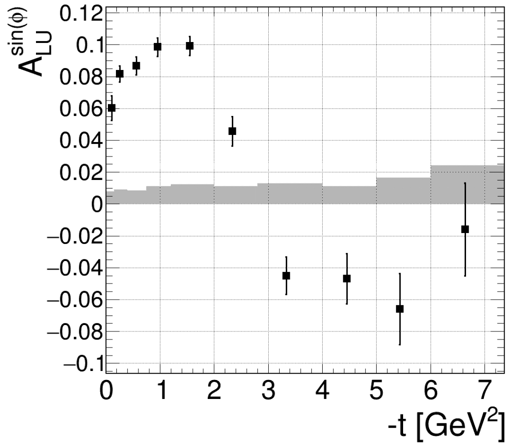

Figure 2: $A_{LU}^{\sin\phi}$ as function of $-t$. The shaded area represents the systematic uncertainty of the measurement. The figure is taken from [13].

3 A multidimensional study in the GPD regime with CLAS12

Based on the new CLAS12 (CEBAF Large Acceptance Spectrometer for experiments at 12 GeV) [19] data, a detailed multidimensional study of $\sigma_{LT'}/\sigma_0$ has been performed in the GPD regime. The experiment uses a longitudinally polarized electron beam, with an energy of 10.6 GeV, interacting with an unpolarized liquid hydrogen target. The CLAS12 forward detector consists of six identical sectors within a toroidal magnetic field. The momentum and the charge of the particles were determined by 3 regions of drift chambers. The electron identification was based on a lead-scintillator electromagnetic sampling calorimeter in combination with a Cherenkov counter. Positive pions were identified by time-of-flight measurements. Cuts on $Q^2 > 1$ GeV^2 and $W > 2$ GeV were applied. The exclusive $e'\pi^+n$ events are selected from the detected electron and π^+ by a cut around the neutron peak in the $e\pi^+X$ missing mass spectrum and the background is subtracted on a bin by bin basis.

Figure 3 shows the Q^2 vs x_B distribution and the applied binning scheme for these variables. The extraction of the beam spin asymmetry follows the methods described for CLAS in

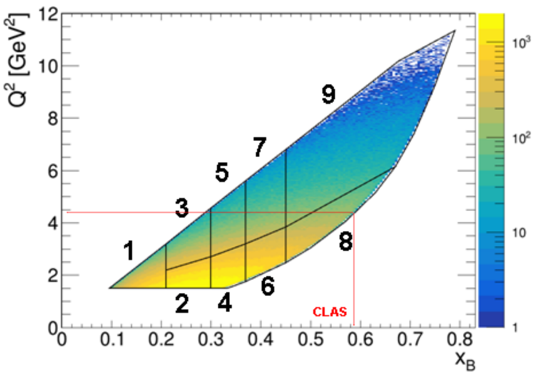

Figure 3: Q^2 vs x_B distribution accessible with CLAS12. The black lines and the numbers indicate the binning scheme used for the multidimensional study. The red line illustrates the region which was accessible with CLAS.

section 2. The results for $\sigma_{LT'}/\sigma_0$ in the region of $-t$ up to 1.2 GeV^2 ($-t/Q^2 \ll 1$), where the leading-twist GPD framework is applicable are shown in Fig. 4. The theoretical predictions from the GPD-based model by Goloskokov and Kroll [17] are shown as a blue line. The

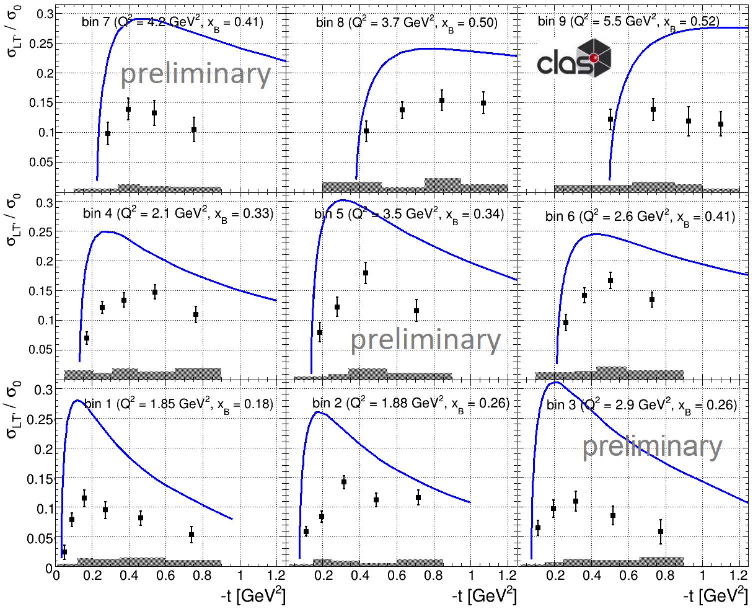

Figure 4: $\sigma_{LT'}/\sigma_0$ as function of $-t$ for different Q^2-x_B bins according to the binning scheme shown in Fig. 3. The gray histogram shows a preliminary estimate of the systematic uncertainty. The blue line shows the predictions from the GK model [17] at the stated mean value of the bins kinematics.

multidimensional study allows a more detailed investigation of the Q^2 and x_B dependence of $\sigma_{LT'}/\sigma_0$ and a precise comparison to the theory predictions in the different kinematic regions. The comparison with predictions from the GPD based GK model [17] shows, that while the magnitude is overestimated by the model, the general slope of the t-dependence and its variation between the single Q^2-x_B bins shows a similar but especially at low Q^2 not fully identical behavior between the model and the experimental results. The mismatch of the amplitude can be interpreted as an indication for an underestimated magnitude of the so far poorly known GPD H_T which is amplified by the interplay with the pion pole term.

4 Conclusion

In summary, the initial study based on CLAS data, provided an extraction of $A_{LU}^{\sin\phi}$ for $\vec{e}p \to e'n\pi^+$ at large photon virtuality, above the resonance region over the full range of kinematics in $-t$, covering the complete kinematic region of the GPD and TDA frameworks simultaneously. A clear sign change of $A_{LU}^{\sin\phi}$ has been observed, indicating a transition from the GPD to the TDA regime. This data-set will help to develop reaction mechanisms for a description of the full kinematic region. Based on the new CLAS12 data it became possible for the first time to do a more detailed multidimensional study of $\sigma_{LT'}/\sigma_0$ in the GPD regime, which allowed an investigation of the Q^2 and x_B dependence of the results. A comparison with predictions from the GPD based GK model [17] showed, that while the magnitude is overestimated, the general slope of the t-dependence and its variation in the single Q^2-x_B bins shows a similar but not fully identical behavior in experiment and theory. The mismatch of the amplitude can be seen as an indication for an underestimated magnitude of the so far poorly known GPD H_T. In combination with previous and future cross section measurements and results from the π^0 and η channels, the presented data will help to better constrain this poorly known GPD in an extended kinematic range. Once more data becomes available from CLAS12 detailed multidimensional studies of the TDA regime will follow.

Acknowledgements

We acknowledge the outstanding efforts of the staff of the Accelerator and the Physics Divisions at Jefferson Lab in making this experiment possible. The authors want to thank P. Kroll, B. Pire, K. Semenov-Tian-Shansky and L. Szymanowski for many fruitful discussions concerning the interpretation of our results.

Funding information This work was supported in part by the U.S. Department of Energy, the National Science Foundation (NSF), the Italian Istituto Nazionale di Fisica Nucleare (INFN), the French Centre National de la Recherche Scientifique (CNRS), the French Commissariat pour l′Energie Atomique, the UK Science and Technology Facilities Council, the National Research Foundation (NRF) of Korea, the Helmholtz-Forschungsakademie Hessen für FAIR (HFHF) and the Ministry of Science and Higher Education of the Russian Federation. The Southeastern Universities Research Association (SURA) operates the Thomas Jefferson National Accelerator Facility for the U.S. Department of Energy under Contract No. DE-AC05-06OR23177.

References

[1] D. Müller, D. Robaschik, B. Geyer, F.-M. Dittes and J. Hořejši, *Wave Functions, Evolution Equations and Evolution Kernels from Light-Ray Operators of QCD*, Fortschr. Phys. **42**, 101 (1994), doi:10.1002/prop.2190420202.

[2] A. V. Radyushkin, *Scaling limit of deeply virtual compton scattering*, Phys. Lett. B **380**, 417 (1996), doi:10.1016/0370-2693(96)00528-X.

[3] X. Ji, *Gauge-Invariant Decomposition of Nucleon Spin*, Phys. Rev. Lett. **78**, 610 (1997), doi:10.1103/PhysRevLett.78.610.

[4] S. V. Goloskokov and P. Kroll, *Transversity in hard exclusive electroproduction of pseudoscalar mesons*, Eur. Phys. J. A **47**, 112 (2011), doi:10.1140/epja/i2011-11112-6.

[5] G. R. Goldstein, J. Osvaldo Gonzalez Hernandez and S. Liuti, *Flexible parametrization of generalized parton distributions: The chiral-odd sector*, Phys. Rev. D **91**, 114013 (2015), doi:10.1103/PhysRevD.91.114013.

[6] M. Diehl and W. Kugler, *Next-to-leading order corrections in exclusive meson production*, Eur. Phys. J. C **52**, 933 (2007), doi:10.1140/epjc/s10052-007-0423-3.

[7] L. L. Frankfurt, P. V. Pobylitsa, M. V. Polyakov and M. Strikman, *Hard exclusive pseudoscalar meson electroproduction and spin structure of the nucleon*, Phys. Rev. D **60**, 014010 (1999), doi:10.1103/PhysRevD.60.014010.

[8] B. Pire and L. Szymanowski, *QCD analysis of $\bar{p}N \to \gamma^* \pi$ in the scaling limit*, Phys. Lett. B **622**, 83 (2005), doi:10.1016/j.physletb.2005.06.080.

[9] B. Pire and L. Szymanowski, *Hadron annihilation into two photons and backward virtual Compton scattering in the scaling regime of QCD*, Phys. Rev. D **71**, 111501 (2005), doi:10.1103/PhysRevD.71.111501.

[10] J. P. Lansberg, B. Pire and L. Szymanowski, *Hard exclusive electroproduction of a pion in the backward region*, Phys. Rev. D **75**, 074004 (2007), doi:10.1103/PhysRevD.75.074004.

[11] K. Park et al., *Hard exclusive pion electroproduction at backward angles with CLAS*, Phys. Lett. B **780**, 340 (2018), doi:10.1016/j.physletb.2018.03.026.

[12] W. B. Li et al., *Unique Access to u-Channel Physics: Exclusive Backward-Angle Omega Meson Electroproduction*, Phys. Rev. Lett. **123**, 182501 (2019), doi:10.1103/PhysRevLett.123.182501.

[13] S. Diehl et al., *Extraction of Beam-Spin Asymmetries from the Hard Exclusive π^+ Channel off Protons in a Wide Range of Kinematics*, Phys. Rev. Lett. **125**, 182001 (2020), doi:10.1103/PhysRevLett.125.182001.

[14] D. Dreschsel and L. Tiator, *Threshold pion photoproduction on nucleons*, J. Phys. G: Nucl. Part. Phys. **18**, 449 (1992), doi:10.1088/0954-3899/18/3/004.

[15] M. Diehl and S. Sapeta, *On the analysis of lepton scattering on longitudinally or transversely polarized protons*, Eur. Phys. J. C **41**, 515 (2005), doi:10.1140/epjc/s2005-02242-9.

[16] T. Arens, M. Diehl, O. Nachtmann and P. V. Landshoff, *Some tests for the helicity structure of the pomeron in ep collisions*, Z.Phys. C **74**, 651 (1997), arXiv:hep-ph/9605376.

[17] S. V. Goloskokov and P. Kroll, *An attempt to understand exclusive π^+ electroproduction*, Eur. Phys. J. C **65**, 137 (2009), doi:10.1140/epjc/s10052-009-1178-9.

[18] B. A. Mecking et al., *The CEBAF large acceptance spectrometer (CLAS)*, Nucl. Instr. Meth. A **503**, 513 (2003), doi:10.1016/S0168-9002(03)01001-5.

[19] V. D. Burkert et al., *The CLAS12 Spectrometer at Jefferson Laboratory*, Nucl. Instr. Meth. A **959**, 163419 (2020), doi:10.1016/j.nima.2020.163419.